Speeding up imaging over BP for automotive radar
High-resolution algorithm with multi-frame data

Yuan, Sen; Fioranelli, Francesco; Yarovoy, Alexander

DOI
10.23919/EuRAD61604.2024.10734973

Publication date
2024

Document Version
Final published version

Published in
Proceedings of the 2024 21st European Radar Conference (EuRAD)

Speeding up imaging over BP for automotive radar: High-resolution algorithm with multi-frame data

Sen Yuan#1, Francesco Fioranelli#2, Alexander Yarovoy#3
#Microwave Sensing Signals & Systems (MS3) Group, Department of Microelectronics, TU Delft, The Netherlands
{1S.Yuan-3, 2F.Fioranelli, 3A.Yarovoy}@tudelft.nl

***Abstract*— One of the key problems in automotive radar is its limited cross-range resolution, despite many approaches developed to address this. Conventional high-resolution algorithms in synthetic aperture radar (SAR) can provide good resolution imaging ability but suffer from high computational costs. In this paper, a computationally efficient high-resolution imaging algorithm is proposed, easing its potential implementation for higher throughput. The proposed approach is verified with experimental data of realistic driving scenarios.**

***Keywords*— MIMO array, direction of arrival estimation, high-resolution imaging, automotive radar.**

I. INTRODUCTION

RADAR can provide accurate and direct measurements of the range, relative velocity, and angle of multiple targets, as well as a long-range coverage even in challenging weather or lighting conditions [1], outperforming in this sense other sensors, namely, camera and Lidar. However, one of the key problems when using radar for automotive is its limited spatial resolution.

To obtain *high spatial resolution*, large-aperture antenna arrays are created either via phased array, or synthetic aperture radar (SAR) [2], or multiple-input-multiple-output (MIMO) techniques [3]. Phased arrays typically use many half-wavelength spaced antennas to form a large aperture with a narrow beamwidth. However, they are not a feasible option for automotive applications. SAR utilizes the variations in the relative Doppler frequency shift of scatterers at different look-angles with respect to the radar trajectory. This forms a large effective (i.e., virtual) aperture array by moving a small physical antenna or array. This reduces the number of physical antennas required for imaging. MIMO approaches can provide a good resolution with few antenna elements, becoming one of the most popular techniques in automotive radar.

In MIMO radar with a virtual uniform linear array (ULA), angle finding can be implemented with a single frame data via digital beamforming (DBF) [4] by performing computationally efficient FFTs on snapshots taken across the array elements or using computationally intensive super-resolution methods, such as Minimum Variance Distortionless Response (MVDR) [5], and subspace-based methods, such as MUltiple SIgnal Classification (MUSIC) and Estimation of Signal Parameters via Rational Invariance Techniques (ESPRIT) [6]. In SAR techniques, all the available data are used during the movement of the radar; hence, more information on targets is available than single-frame data. This often leads to better resolution than in MIMO algorithms. Many researchers try to combine both advantages together in MIMO-SAR algorithms [7]–[10], using back-projection (BP) as the fundamental basis of such methods. However, back-projection is a heavily time-consuming algorithm, which adds coherently all the signals together, although some efficient implementations have been proposed [11].

Our previous study [12] proposed the idea of a 'motion-enhanced snapshot' to perform direction of arrival (DOA) estimation using limited snapshots. The concept is further extended to 3D imaging [13] only using 1D array in automotive applications. However, this method uses only one data frame, which limits its imaging ability. To improve imaging but yet maintain computational efficiency, this paper proposes an efficient, high-resolution imaging algorithm by incoherently adding the target information over multiple frames. This extends the limits of the method in [13] and provides comparable results as BP with less computational costs; the proposed method is validated with experimental data in realistic driving scenarios.

The rest of the paper is organized as follows. Section II briefly summarizes fundamental concepts to introduce the proposed method in Section III. Results are presented in Section IV, with conclusions drawn in Section V.

II. FUNDAMENTALS

A. Signal Model

The received signal is the superposition of the signals reflected by targets in the field of view as:

$$\begin{aligned} z(i,l,k) = &\sum_{o=1}^{K} \alpha_o exp[j2\pi f_0 \frac{id}{c} sin\theta_o] \\ &\times exp[-j4\pi f_0 \frac{D_o(l)}{c} + \mu \frac{2\pi D_o(l)(k-1)}{cf_s}] \end{aligned} \tag{1}$$

where z indicates the digitized signal; i is the index of antenna elements counted in the virtual ULA relative to the 1^{st} antenna element; $l = \lfloor \frac{t}{T} \rfloor$ with $t' = t - lT$ where T is the pulse repetition interval; $t' \in [0, T_c]$ with $i = 0, 1, 2, ..., I-1$ where I is the total number of antenna elements in the array, and T_c is the chirp duration; $k = 0, 1, 2, ..., K_d - 1$ where $K_d = T_c f_s$ is the maximum number of samples within one chirp and f_s is the fast time sampling frequency; $l = 0, 1, 2, ..., L_d - 1$ is the slow time index; L_d is the total number of chirps in one frame; o is the index of the discretized cells; K is the total number of cells; α_o is the complex amplitude related to the target characteristics in cell o; f_0 is the chirp starting frequency; d is the space interval between adjacent antenna elements; c is the speed of light; θ_o is the azimuth of cell o; μ is the frequency modulation rate; D_o is the distance between antenna & cell o.

B. BP algorithm

For each discretized imaging grid cell (x_o, y_o), the range to the antenna is:

$$D_o(l) = \sqrt{(x_o - \frac{v_x(l-1)}{T_c})^2 + (y_o - \frac{v_y(l-1)}{T_c})^2} \quad (2)$$

The first step of BP is to perform an interpolated fast Fourier transform (FFT) along the dimension of the fast time to obtain a high-resolution range profile for each chirp. Thus, the first antenna's signal $Z(l,k)$ derived from 2D slices of the tensor $z(1,:,:)$ in (1) are used for later processing. $Z_{\hat{r}} = FZ$, where F is the interpolated FFT matrix. Then, the values of the corresponding cells in the range profile are selected based on the distance from each grid cell to the radar. The extra phase term is compensated according to the distance for each signal, and the compensated results are accumulated to obtain the scattering information at the grid. The scatter information can be obtained as follows:

$$X(x_o, y_o) = \sum_{l=0}^{L_d-1} Z_{\hat{r}}(\mathbf{idx}(n), l) exp(\frac{j4\pi f_c D_o(l)}{c}) \quad (3)$$

where $\mathbf{idx}(n) = round(\frac{2\alpha B}{c} R_o(n))$ is the index of cell o and α the interpolation factor. The phase term is the compensated phase for the cell o. After each cell is calculated, the BP results can be obtained.

In automotive radar, the received signals are collected frame by frame. The frame index is defined as $f = 0, 1, 2, ..., F-1$. The frame time is T_f. BP algorithm can deal with this easily by considering the movement in multiple frames. The equation (2) will change as:

$$D_o(l,f) = \sqrt{\begin{matrix}(x_o - v_x(f)(l-1)T_c - v_x(f)(f-1)T_f)^2 \\ +(y_o - v_y(f)(l-1)T_c - v_y(f)(f-1)T_f)^2\end{matrix}} \quad (4)$$

C. Motion-enhanced imaging algorithm

3D imaging algorithm using a 1D MIMO array for one-frame data processing is proposed in [13]. The algorithm uses motion-enhanced snapshots to achieve high angular resolution for automotive radar. With the aforementioned signal model, for the discretized grid cell (x_o, y_o), the range to the antenna can be written as:

$$D_o(l) = R_o + v_r T_c(l-1) \quad (5)$$

When $D_o(l_1) - D_o(l_2) = d\sin\theta_{\mathbf{o}}\cos\phi_{\mathbf{o}}$, the antenna is physically moved to a new position in half wavelength intervals. A larger aperture can, therefore, be formed by these motion-enhanced snapshots. It follows that:

$$\begin{aligned} d\sin\theta_{\mathbf{o}}\cos\phi_{\mathbf{o}} &\approx v_y \sin\theta_{\mathbf{o}}\cos\phi_{\mathbf{o}} \mathrm{T_c}(\mathrm{l_1} - \mathrm{l_0}) \\ \Rightarrow l_1 &= l_0 + \lfloor \frac{d}{2v_y T} \rfloor T \end{aligned} \quad (6)$$

where the approximation is because the major velocity component for the vehicle is in the forward direction, which is the same direction as the antenna array for side-looking radar. For this, a formulation of the steering vector is proposed to address the 3D imaging problem jointly in azimuth & elevation and to compensate motion artefacts from the irregular movement of the vehicle, detailed in [13].

III. Problem formulation and proposed method

The BP algorithm can provide robust high-resolution images in a 2D plane. However, since it accumulates multiple frame data for each grid cell to form an image, it is computationally expensive, limiting its real-time application. The motion-enhanced imaging algorithm provides a lower computational cost solution to 3D high-resolution imaging. However, as the movement of the car in one snapshot is limited, it is hard to interpret the environment with such little information.

To address this gap and improve imaging capabilities while maintaining computational efficiency, an efficient, high-resolution imaging algorithm is proposed. This uses weighted incoherent summation with multi-frame motion-enhanced imaging data. The grid cell is divided according to global coordinates at first. Then, each cell of the observation region will be contributed by every frame data containing the information of this cell using the vehicle motion. Specifically, the weight parameter is defined as:

$$w(x_o, y_o) = exp(-abs(\theta_o)) \quad (7)$$

This decreases with the direction of arrival angles; the farther from the broadside, the less weight. The weight parameter not only takes into consideration the fact that resolution is higher in the broadside view than in other directions but also provides different weight contributions among multi-frame data, i.e., for a given position in the observation region, the frame data observing in the broadside needs to be trusted more with high weight. The flowchart of the proposed method compared with the conventional BP algorithm is shown in Fig.1.

IV. Results

The proposed approach is verified with experimental data. The radar used is the TI AWRx cascade model, mounted on the top side of the vehicle shown in Fig. 2. The radar is installed next to a GoPro camera, while a Lidar is on the top-middle of the car. The radar operates at 77GHz. The radar parameters are specified as follows: the starting frequency of the chirp f_0 is 77 GHz, the chirp bandwidth B is 1.28 GHz, the chirp

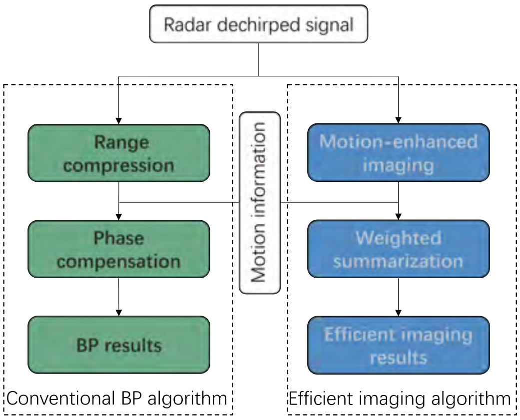

Fig. 1. The proposed efficient imaging algorithm compared with conventional BP algorithm

duration T_c is 43 μs, the sampling rate f_s is 60 Msps, and L = 128 chirps are processed in each frame. The MIMO antenna on the forward-looking radar is located at the coordinate centre.

Fig. 2. Car with multiple sensors used for the data collection

The following figures present images captured by different sensors for comparison in the same scenarios. In Fig. 3(a), imagery from a GO-pro camera offers an empirical interpretation of the scenario, with key targets such as a bus stop, rubbish bin, and display marked. Fig. 3(b) shows the point cloud from Lidar sensors for the same scenarios. The point cloud is dense enough to provide a comprehensive understanding of the surroundings.

Fig. 4 demonstrates the results obtained from radar data using different algorithms. Fig. 4(a) is based on one single snapshot with one antenna element in azimuth direction using the original algorithm proposed in [13]. The two cars are separated successfully in the image. However, due to the limited movement and limited data available within one frame duration, it is still hard to interpret the image. Fig. 4(b) is obtained by the conventional BP algorithm using 49 data frames. The two cars have more detailed contours in the formed images. The entrance of the building is clear in the

(a)

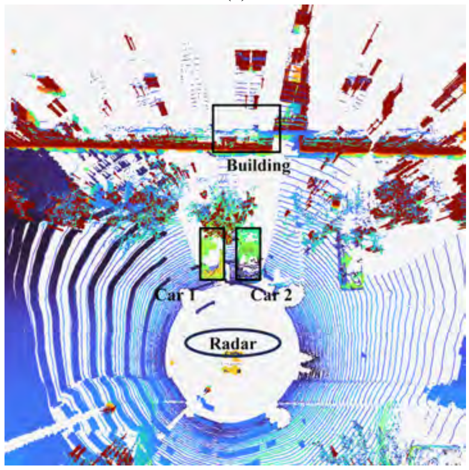

(b)

Fig. 3. (a) The optical image from the camera. (b) The point cloud image from Lidar

radar images as well, making it easier for later radar-based applications, i.e., classification and mapping. Fig. 4(d) is the result of the efficient imaging algorithm using 49 frames as well as the proposed weight function, whereas Fig. 4(c) shows the result without weight.

All the tests are performed on a Dell OptiPlex 7060 PC with Intel i5-8500 CPU. The conventional BP algorithm takes 70.67s to generate the BP image, while the efficient imaging algorithm only takes 20.05s, speeding up 3.5 times in the computation. The reduced computational cost is mainly due to the avoidance of interpolation during the BP phase compensation and energy searching for each chirp among all frames.

These visual comparisons show that both algorithms can provide enough information about the two cars, buildings and the entrance. The weight function helps redistribute the energy among the close targets, which increases the resolution ability. Theoretically speaking, the BP algorithm can provide larger apertures than the proposed efficient imaging algorithm. The aperture formed by BP for the target equals to $\frac{D}{2R}$ where D is the width of the radar beam, and R is the range between the radar trajectory and the target. The efficient imaging algorithm can provide an aperture equal to the physical movement of the radar during one frame of time. However, with accumulated information among all the frame data, a better image can be

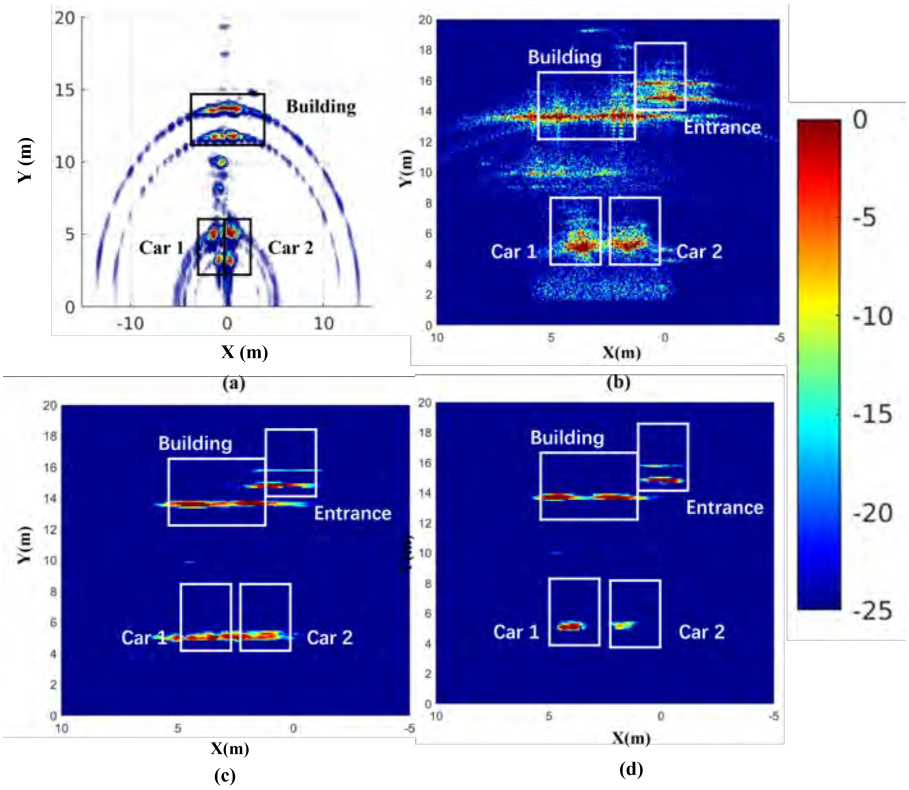

Fig. 4. The radar imaging results: (a) single snapshot imaging results using [13], (b) conventional BP imaging results, (c) efficient imaging results without weight function, (d) efficient imaging results with weight function.

generated.

V. Conclusion

In this paper, an efficient, high-resolution imaging algorithm for automotive radar using multiple frame data is proposed. The algorithm can perform three times faster compared with the conventional BP algorithm, which is important for future real-time applications in automotive systems. The proposed approach is verified with experimental data collected in realistic driving scenarios.

Acknowledgment

The authors would like to thank the China Scholarship Council for the PhD scholarship of S. Yuan, and are also grateful to I. Roldan, A. Palffy, and the joint team of the MS3 and Intelligent Vehicles (IV) groups of TU Delft for organizing the experimental data collection and making them available.

References

[1] F. Engels, P. Heidenreich, A. M. Zoubir, F. K. Jondral, and M. Wintermantel, "Advances in automotive radar: A framework on computationally efficient high-resolution frequency estimation," *IEEE Signal Processing Magazine*, vol. 34, no. 2, pp. 36–46, 2017.

[2] Y. K. Chan and V. C. Koo, "An introduction to synthetic aperture radar (sar)," *Progress In Electromagnetics Research*, vol. 2, pp. 27–60, 2008.

[3] E. Biglieri, R. Calderbank, A. Constantinides, A. Goldsmith, A. Paulraj, and H. V. Poor, *MIMO wireless communications*. Cambridge university press, 2007.

[4] P. Barton, "Digital beam forming for radar," *IEE Proceedings F (Communications, Radar and Signal Processing)*, vol. 127, pp. 266–277(11), August 1980.

[5] J. Capon, "High-resolution frequency-wavenumber spectrum analysis," *Proceedings of the IEEE*, vol. 57, no. 8, pp. 1408–1418, 1969.

[6] R. Roy and T. Kailath, "Esprit-estimation of signal parameters via rotational invariance techniques," *IEEE Transactions on Acoustics, Speech, and Signal Processing*, vol. 37, no. 7, pp. 984–995, 1989.

[7] B. Zhang, G. Xu, R. Zhou, H. Zhang, and W. Hong, "Multi-channel back-projection algorithm for mmwave automotive mimo sar imaging with doppler-division multiplexing," *IEEE Journal of Selected Topics in Signal Processing*, 2022.

[8] S. Yuan, F. Fioranelli, and A. Yarovoy, "3drudat: 3d robust unambiguous doppler beam sharpening using adaptive threshold for forward-looking region," *IEEE Transactions on Radar Systems*, 2024.

[9] S. Yuan, P. Aubry, F. Fioranelli, and A. G. Yarovoy, "A novel approach to unambiguous doppler beam sharpening for forward-looking mimo radar," *IEEE Sensors Journal*, vol. 22, no. 23, pp. 23 494–23 506, 2022.

[10] M. Manzoni, D. Tagliaferri, M. Rizzi, S. Tebaldini, A. V. M. Guarnieri, C. M. Prati, M. Nicoli, I. Russo, S. Duque, C. Mazzucco *et al.*, "Motion estimation and compensation in automotive mimo sar," *IEEE Transactions on Intelligent Transportation Systems*, vol. 24, no. 2, pp. 1756–1772, 2022.

[11] M. Hoffmann, T. Noegel, C. Schüßler, L. Schwenger, P. Gulden, D. Fey, and M. Vossiek, "Implementation of real-time automotive sar imaging," *arXiv preprint arXiv:2306.09784*, 2023.

[12] S. Yuan, F. Fioranelli, and A. Yarovoy, "Vehicular motion-based doa estimation with a limited amount of snapshots for automotive mimo radar," *IEEE Transactions on Aerospace and Electronic Systems*, 2023.

[13] ——, "3d high-resolution imaging algorithm using 1d mimo array for autonomous driving application," 2024.